Fluid Patterns and Time-Dependent Driving

Tuesday, Sept. 1: 11:00 – 13:00

Session 3: MPI Lecture Hall

Contents

1

Miscible viscous fingering in porous media: influence on adsorbed solute dynamics

M. Mishra[1], M. Martin[2], and A. De Wit[1]

[1] Nonlinear Physical Chemistry Unit, Université Libre de Bruxelles, Brussels, Belgium
[2] PMMH, Ecole Supérieure de Physique et de Chimie Industrielles, Paris, France

Miscible viscous fingering (VF) is an interfacial fluid flow instability that occurs when a less viscous fluid displaces another more viscous miscible one in a porous medium, leading to the formation of finger like patterns at the interface of both fluids [1]. VF impacts a variety of practical applications such as oil recovery, filtration and hydrology, liquid chromatography, and even medical applications. In liquid chromatography (LC), which is used to separate the chemical components of a sample by passing it through a porous medium, VF can be of concern when the sample solvent has a viscosity different from that of the displacing fluid [2, 3]. The possible adsorption of solutes or analytes onto the porous matrix can affect their concentration pattern because of this VF leading to anomalous peak shapes in reversed-phase liquid chromatography [4]. Here, we investigate numerically the influence of VF due to the difference in sample solvent and displacing fluid viscosities on the evolution of a solute initially contained in the sample. To do so, we study a three component system by considering Darcy's law for the fluid velocity coupled with a mass-balance equation for the sample solvent and solute concentrations. A linear isotherm model is used for the adsorption of the passive solute onto the porous matrix. The influence of parameters that control VF and especially of the retention parameter κ' is analyzed.

We investigate in particular the conditions for disengagement of the retained solute zone with respect to the sample solvent zone. Density plots of solute concentration fields for different retention parameters κ' are plotted at successive times in Fig.1.1. VF occurs because the displacing fluid has a lower viscosity than the sample solvent. If $\kappa' = 0$, the VF pattern of the unretained solute is the same as that of the solvent (Fig.1.1a). In the presence of adsorption the retained solute develops fingering of its distribution zone at either the rear or frontal interface or on both of them when in contact with the unstable interfaces of the sample solvent zone (Figs.1.1b-c). This retained analyte zone disengages rapidly from the sample solvent zone for large values of κ' giving then barely no distortion at both interfaces (see Fig.1.1d). These results are analyzed quantitatively through computation of the various moments of the concentration distributions [1, 2]. The time interval between the onset time of viscous fingering effects on the analyte plug and the time of saturation (complete disengagement of the sample plug) is decreasing with increasing κ'. So, the larger κ', the quicker the separation of both analyte and sample solvent plugs and the less detrimental the influence of VF on the spreading of the solute. These results are in agreement with recent experimental findings in chromatography [4].

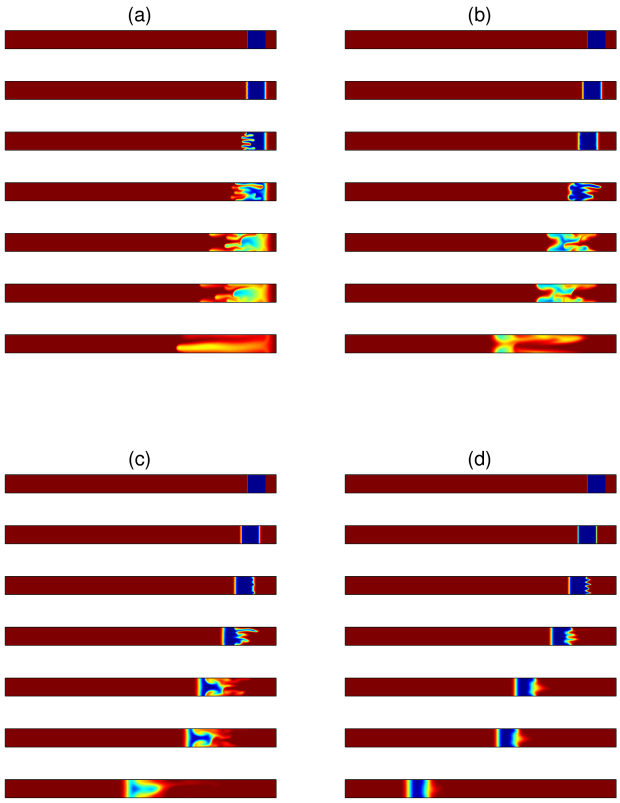

Fig. 1.1: Evolution of the solute concentration at successive times in a frame moving at the velocity of the eluent with (a) $\kappa' = 0$, (b) $\kappa' = 0.3$, (c) $\kappa' = 0.5$, (d) $\kappa' = 1$.

References

1. G. M. Homsy, Viscous fingering in porous media, Ann. Rev. Fluid Mech. **19**, 271, (1987).
2. A. De Wit, Y. Bertho, and M. Martin, Viscous fingering of miscible slices, Phys. Fluids **17**, 054114 (2005).
3. M. Mishra, M. Martin, and A. De Wit, Miscible viscous fingering with linear adsorption on the porous matrix, Phys. Fluids **19**, 073101 (2007).
4. S. Keunchkarian, M. Reta, L. Romero, and C. Castells, Effect of sample solvent on the chromatographic peak shape of analytes eluted under reversed-phase liquid chromatographic conditions, J. Chromatogr. A **1119**, 20 (2006).

2

Convection in colloidal suspensions

M. Gläßl, M. Hilt, and W. Zimmermann

Theoretische Physik, Universität Bayreuth, D-95440 Bayreuth

Thermal convection in colloidal suspensions is described by a generalized continuum model for binary fluid mixtures, considering additional terms unaccounted in Boussinesq approximation. Via the Soret effect an external temperature gradient induces a gradient of the density of particles.

Depending on the suspended particles this concentration gradient may lead to spatial variations of the shear viscosity as well as of the thermal conductivity of the mixture. Both dependencies change the onset and the nonlinear properties of convection. A density dependent thermal conductivity leads, for instance, in a certain range of material parameters to a restabilization of the nonlinear conductive state.

Thermosensitive colloidal particles change their size during the convective motion from warmer to colder volumes in the cell. We describe this behavior by introducing a temperature dependent Lewis number and discuss the resulting effects on convection.

3

The Rayleigh-Plateau instability on a polymeric viscoelastic filament

R. Sattler[1], C. Wagner[1], and J. Eggers[2]

[1] Experimentalphysik, Universität des Saarlandes, Postfach 151150, 66041 Saarbrücken, Germany
[2] School of Mathematics, University of Bristol, University Walk, Bristol BS8 1TW United Kingdom

When a drop falls from a faucet, surface tension drives the fluid motion toward breakup in finite time, and a drop separates. This pinch-off occurs in a localized fashion, and the neighborhood of the point of breakup is described by a similarity solution [1]. If however very small amounts of high molecular weight polymer are added, an almost perfectly cylindrical thread is formed instead. The reason is that wherever there is a local decrease in radius, fluid elements are stretched, and the polymers along with it. This will increase the extensional viscosity of the fluid-polymer mixture, and further flow is inhibited, thus forming a uniform and stable filament that thins exponentially in time.

Theoretically, the period of exponential thinning has recently been described within a long-wavelength description [2]. Nonetheless, the full three-dimensional, axisymmetric problem remains unsolved. The effect of finite polymer extensibility has been studied numerically in [3], once more using a long-wavelength model. The filament is found to fail near its end via a localized similarity solution, in contrast to the much more complex scenario found here.

The observations we report here have general validity for a variety of polymer-solvent systems. Experiments have been performed with polyethylenoxide (PEO) in water, PEO in xylol, human saliva, polyacryl-co-acrylicacid in water-sugar, polysterol in diethyl phthalate and dimethyl furane.

For plug flow in a cylindrical filament, the elongation rate is determined from $\dot{\epsilon} = -2d\ln h/dt$, thus $\dot{\epsilon}$ is constant for most of the filament thinning, which follows an exponential law. The axial stress σ_{zz} supported by the polymers balances the increasing capillary pressure γ/h_{min}, which means that the extensional viscosity $\eta_E \equiv \sigma_{zz}/\dot{\epsilon} = \gamma/(h_{min}\dot{\epsilon})$ also increases exponentially. Once η_E has reached a plateau, which we estimate at $h_{min} \approx 12\mu m$ to be $\eta_E\,(12\mu m) \approx 330Pas$, the filament behaves essentially like a Newtonian fluid [3], and is thus subject to a capillary instability [1]. Note that this value of the extensional viscosity corresponds to an increase by 5 orders of magnitude over $\eta_{water} = 10^{-3}Pas$ of the solvent.

The *linear* instability which is shown in Fig. 3.1 evolves when the thinning process has become to a rest. At first, no oscillations are visible on the images of Fig. 3.1; however, we are able to resolve perturbations down to an amplitude of $A = 80nm$, corresponding to significant super-resolution. Over more than a decade, the growth is very well described by an exponential, providing a clear signature of a *linear instability*, which develops uniformly in space.

From a fit to the exponential, we find an inverse growth rate of $1/\omega = 9.3 \pm 0.1ms$. Linear stability of a viscous fluid thread [1] predicts $\omega = \gamma/(6R_0\eta_{eff})$,

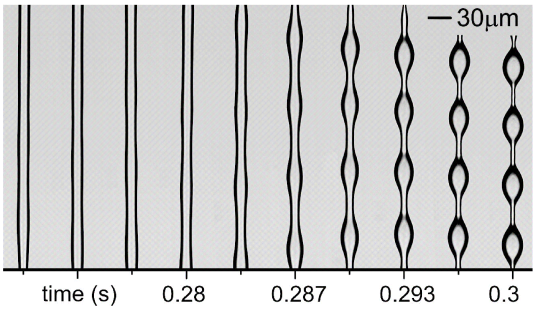

Fig. 3.1: Growth of a sinusoidal instability of the viscoelastic filament that develops into a group of droplets on the thinning filament. The spacing of the pictures is $300^{-1}s$.

which gives an estimated extensional viscosity of $\eta_{eff} = 9Pas \pm 2$. At the same time, we are able to fit - as expected [1] - a *linear* law $h_{min} = -0.44 \times 10^{-3}m/s\Delta t$ in the range $8\mu m > h_{min} > 4\mu m$. Comparing to the law $h_{min} = 0.07\gamma/\eta_{eff}\Delta t$ for viscous pinching [4], this gives $\eta_{eff} = 10Pas$, which agrees nicely.

If the polymer concentration was greater than 1000 ppm, the filament connecting two beads *never* breaks. In other words, the thin filament must have formed a (solid) phase different from that of the drops To confirm this idea, we produced the Scanning-Electron-Microscopy (SEM) images that allowed us to estimate the diameter of the fiber as $75 - 150nm$.

References

1. J. Eggers, Rev. Mod. Phys. **69**, 865 (1997).
2. C. Clasen, J. Eggers, M.A. Fontelos, J. Li, and G.H. McKinley, J. Fluid Mech. **556**, 283 (2006).
3. J. Li and M.A. Fontelos, Phys. Fluids **15**, 922 (2003).
4. A. Rothert, R. Richter, and I. Rehberg, *New Journal of Physics* **5**, 59.1 (2003).

4

Spatial forcing in inclined layer convection

S. Weiss[1], G. Seiden[1], and E. Bodenschatz[1,2]

[1] Max Planck Institute for Dynamic and Self-Organization, D-37073 Göttingen, Germany
[2] Department of Physics, Cornell University, Ithaca, New York 14853-2501, USA

Naturally driven pattern forming systems often contain externally imposed symmetry breaking mechanisms that affect the occuring patterns and their dynamics. Frost heave phenomena leading to stone-soil separation in alpine and polar regions or the formation of vegetation stripes on hillsides in arid areas are just two examples where an anisotropic boundary (i.e. the sloped ground) determines the observed pattern.

We explore the effect of two independent symmetry breaking elements, imposed on a pattern forming system. As a model, we choose thermal convection, where a thin fluid layer of height d is heated from below and cooled from above. In a horizontal fluid layer, convection sets in at a critical temperature difference ΔT_c. Due to the rotational symmetry of the system, straight parallel convection rolls emerge that are aligned in an arbitrary direction [1]. Tilting the RBC cell, however, breaks the rotational symmetry, resulting in a large scale shear flow. In the resultant inclined layer convection (ILC), the direction of the convection rolls depends on the inclination angle. For inclinations smaller than a critical angle θ_c, the buoyancy driven convection rolls are aligned with their axis parallel to the in-plane gravity component. For $\theta > \theta_c$, the instability is driven by the shear stress due to the large scale shear flow, leading to rolls that are aligned vertical to the gravity component [2].

In addition to the rotational symmetry breaking introduced by inclination, we impose a second symmetry breaking mechanism in the form of microfabricated 1D periodic surface corrugations of the bottom plate (Fig. 4.1a). Both, the relative orientation of these corrugations with respect to the inclination direction (ϕ in Fig. 4.1a) and the corresponding wave number q_f can be varied in the experiment. In addition, by varying the inclination angle θ, and the reduced temperature difference $\epsilon = \Delta T/\Delta T_c - 1$, one can change the intensity of the large scale shear flow and thus, tune the relative strength of the two independent symmetry breaking mechanisms.

In our experiment, we use pressurized CO_2 gas in a large aspect ratio cell. The corresponding Prandtl number of the fluid is Pr=1.30. The fluid is laterally confined by a square cell, aligned with respect to the inclination direction. The temperature field is observed by utilizing the shadowgraph technique [3].

Due to the spatial periodic forcing, a well-defined convection onset cannot exist anymore. Instead, convection rolls with wave number q_f exist for all positive temperature differences ΔT. We focus on the instability of straight rolls and study the pattern that appear for higher values of ϵ. Depending on the forcing scenario, we observe a variety of novel pattern forming processes ranging from stabilization of spatiotemporal chaos to the emergence of novel

two-dimensional patterns. We explore the $\theta - \epsilon$ phase space and present corresponding phase diagrams for ϕ =0°, 60° and 90°. For longitudinal forcing ($\phi = 0°$), a stabilization of pattern and their dynamics in comparison to the unforced case is observed. In the transverse ($\phi = 90°$) and oblique forcing scenarios ($\phi = 60°$), the interaction between the intrinsic modes of the system and the external constraints leads to patterns with a rhombic, an hexagonal or a bimodal structure. Particularly interesting are complex superlattice patterns that occur for large inclination angles (see Fig. 4.1 b and c).

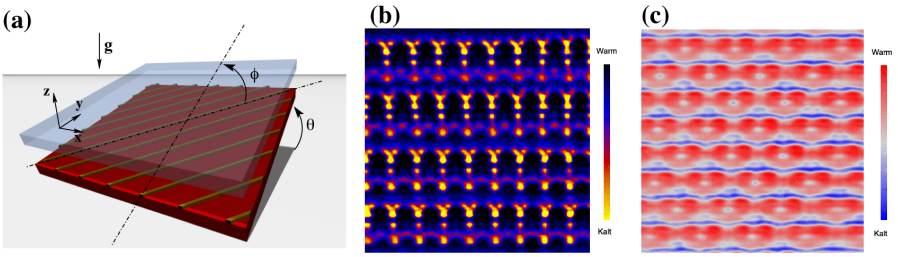

Fig. 4.1: (a) Schematic of the forced inclined layer convection cell. For transverse forcing ($\phi = 90°$), novel superlattice patterns where found as e.g. Scepter Pattern (b) and Heart Pattern (c).

References

1. E. Bodenschatz, W. Pesch, and G. Ahlers. Recent developments in Rayleigh-Bénard convection. *Annu. Rev. Fluid Mech.*, 32:709, 2000.
2. K. Daniels, B. Plapp, and E. Bodenschatz. Pattern formation in inclined layer convection. *Phys. Rev. Lett.*, 84:5320, 2000.
3. J. R. de Bruyn et al. Apparatus for study of Rayleigh-Bénard convection in gases under pressure. *Rev. Sci. Instrum.*, 67:2043, 1996.
4. G. Seiden, S. Weiss, J. McCoy, W. Pesch, and E. Bodenschatz. Pattern forming system in the presence of different symmetry-breaking mechanisms. *Phys. Rev. Lett.*, 101:214503, 2008.

5

Computer simulation for Rayleigh-Bernard instability in finite container

V.V. Kolmychkov, O.S. Mazhorova, and O.V.Shcheritsa

Keldysh Institute of Applied Mathematics RAS, Moscow

Rayleigh-Benard convection, i.e. convection in a horizontal layer heated from below, permanently attracts attention of the researchers as a meaty example of hydrodynamical system in which transition to various types of instabilities can be studied. When the temperature difference between lower and upper plate is large enough, buoyancy forces lead to the destabilization of the quiescent state and convection evolves. The first stable convection pattern takes the form of rolls. The strength of buoyancy forces are determined by Rayleigh number Ra, the size of rolls are described by wave number k. For different values of Prandtl number stability area of roll structures in the plane (Ra, k) has been obtained in [1]. Though RB system has been extensively studied both theoretically and experimentally, there is a lack of quantitative and reliable comparisons between theory and experiment. The paper deals with numerical study of the roll structures stability and producing in calculations overriding types of instabilities theoretically predicted. The process is described by time-dependent Navier-Stokes in Boussinesq approximation.

At first in scope of 2D approach, the region in (Ra, k) plane where rolls are stable is determined and compared with Busse Balloon [2] to estimate the effect of sidewalls. Numerical results show that the presence of sidewalls, no matter how distant, substantially restrict the possible wave-numbers which can occur in the bulk of the system. Near the convective threshold the band of available wave numbers is reduced to a range $|k| \sim (Ra - Ra_{cr})/Ra_{cr}$ instead of a size $|k| \sim [(Ra - Ra_{cr})/Ra_{cr}]^{1/2}$ in the infinite systems. This is compatible with theoretical data [3].

Then the onset of steady roll convection from initial disturbances is studied. Three scenarios of the flow pattern evolution, entitled *stable, quasi stable* and *roll diffusion*, have been registered in calculations. They are described and discussed both in two and three dimensional cases. Also essentially 3D flow pattern evolution has been observed. The calculations show the transition from unsteady rolls to skewed varicose instability (fig. 5.1), oscillatory convection and spiral defect chaos (fig. 5.2).

The simulation is performed using the numerical procedure [4] , which proves it's reliability in calculation of various convective heat and mass transfer problems [5].

References

1. A.Schlüter, D. Lortz, F.Busse, On the stability of steady finite amplitude convection, J. Fluid Mech. **23**(1), 129 (1965)

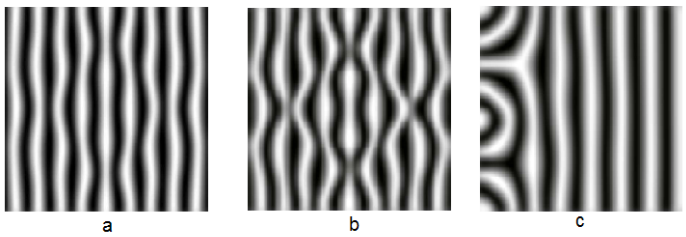

Fig. 5.1: Temperature field in the plane $z = 0.5$ plane. Time evolution of skewed varicose instability.

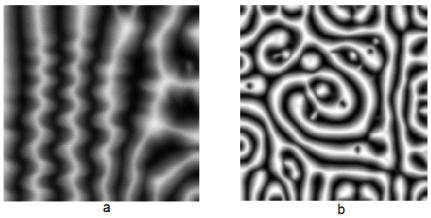

Fig. 5.2: Oscillatory convection and spiral defect chaos.

2. F.H.Busse, R.M.Clever, Instabilities of convection rolls in a fluid of moderate Prandtl number, J. Fluid Mech. **91**(2), 319 (1979).
3. M.C.Cross, P.G.Daniels, P.C.Hohenberg, E.D.Siggia, Phase-winding solution in a finite container above the convection threshold, J. Fluid Mech. **127**, 155 (1983)
4. V.V.Kolmychkov, O.S.Mazhorova, Y.P.Popov, Analysis of Solution Algorithms for the Three-Dimensional Navier-Stokes Equations in the Natural Variables, Differential Equations, **46**(7), 994 (2006)
5. V.V.Kolmychkov, O.S.Mazhorova, Y.P. Popov, P.Bontoux, M.El.Ganaoui, Identification of the convective instability in a multi-component solution by 3D simulations, Comptes Rendus Mecanique, **333**(10), 739 (2005).

6

Phase transition and dynamical properties for one-dimensional Fermi accelerator models

Edson D. Leonel

Departamento de Matemática – Instituto de Geociências e Ciências Exatas
Universidade Estadual Paulista, Av.24A, 1515 – Bela Vista – CEP: 13506-900 –
Rio Claro – SP – Brazil

The main goal of this seminar is to present and discuss some results for one-dimensional accelerator models like Fermi-Ulam [1,2] and Bouncer [3,4] models. We consider both the conservative and dissipative cases and different external perturbations for the boundary. For the conservative case we characterise some scaling properties of chaotic seas obtaining critical exponents for the phase transition: integrability to no integrability. For the dissipative case we show the occurrence of boundary crisis and in particular a phase transition from limited to unlimited energy growth is characterised in the bouncer model.

References

1. E. Fermi, Phys. Rev. **75** (6), 1169 (1949).
2. E. D. Leonel, P. V. E. McClintock, J. K. L. da Silva, Phys. Rev. Lett. **93**, 014101 (2004).
3. A. L. P. Livorati, D. G. Ladeira, and E. D. Leonel, Phys. Rev. E **78**, 056205 (2008).
4. E. D. Leonel, A. L. P. Livorati, Physica A **387**, 1155 (2008).

7

Fly-wheel model of the hither and thither motion of a bouncing ball

Gy. Károlyi[1], A. Bibó[1], and T. Bódai[2]

[1] Department of Structural Mechanics, Budapest University of Technology and Economics, Műegyetem rkp. 3., H-1111 Budapest, Hungary
[2] Centre for Applied Dynamics Research, School of Engineering, University of Aberdeen, King's College, AB24 3UE Aberdeen, Scotland, UK

Collisions are very important in many fields of Nature and Science and have wide-spread applications in industry. In Nature, the impact of ice particles are thought to be related to the formation of Saturn's rings, and the single-particle impacts can play a crucial role in understanding the behaviour of snow or sand avalanches. In Science, the ergodic behaviour of impacting billiard systems is supposed to give ideas to describe the stochasticity of gas and to the Boltzmann hypothesis. In many sports like tennis, golf or baseball it takes years of practice to achieve the desired bounce of the ball with the right speed, angle and spin. Applications of impacting bodies include the use of granular materials in chemical, pharmaceutical, agricultural, mining or mineral processing industry. In computer simulations of granular materials it is desirable to have simple, but accurate models of the interaction forces and impact properties.

In order to construct such models many experimental investigations of impacts have been carried out. Probably the simplest of these experiments concern the oblique collision of balls or disks with a planar surface, with or without initial spin. Parallel with the experimental studies, many models have been formulated to describe oblique impacts. The early attempts considered the impacting ball to be rigid. However, such rigid body models are not capable of describing the observed changes in the direction of the tangential force acting on the contact surface or reversals of the contact point velocity during a single impact of a ball, observed most notably in case of solid rubber balls referred to as "superballs".

It became clear that the elastic deformations must be taken into account for a proper modelling of the tangential forces. In principle, the deformable surface of the impacting ball acts like a "tangential spring" during the collision with the surface. It is the interplay of the repeated stick and slip and the effects of the elastic deformations that causes the complexity of the oblique impact of a ball on a flat surface. As a consequence of this, with some practising, one can throw a ball in such a way, that it "comes back" after the collision with the surface. The ball has to spin "backwards" to achieve this reversal. In fact, it is possible to throw a solid rubber ball (e.g. superball) so that in the first few bounces on a flat horizontal surface it always rebounces, that is, the velocity of its centre of mass and its angular velocity changes direction in each collisions.

In this paper we address this hither and thither motion of an elastic ball, and construct a very simple, low-dimensional model that can exhibit a very similar behaviour. We show that a simple fly-wheel model exhibits the ob-

served to and fro motion of elastic balls. The suggested model is capable of describing oblique impacts of spherical bodies, which can be important in many applications, including dynamical simulation of granular materials. We find that the behaviour of the bouncing fly-wheel is sensitive to the initial conditions, and the escape time plots are used to illustrate this observation and to discover in which parameter and initial value regions the repeated reversals are to be expected.

References

1. A. Bibó, Gy. Károlyi, T. Bódai, Fly-wheel model exhibits the hither and thither motion of a bouncing ball, preprint, 2009.

8

Theoretical results on the Swinging Atwood Machine

A. Aparicio Monforte[1], S. Simon Estrada[2], and J.-A. Weil[1]

[1] Département Maths Informatique, Université de Limoges
XLIM - UMR CNRS n. 6172, 123, avenue Albert Thomas, 87060 Limoges (France)
[2] Department of Mathematics, University of Portsmouth
Lion Gate Building, Lion Terrace, Portsmouth PO1 3HF (United Kingdom)

The **Swinging Atwood's Machine** (SAM) ([5]) is a compound mechanism comprising a pulley and a pendulum and linking two point masses, one of them allowed to swing in a plane. This coupled oscillator, basically a variation of the well-known Atwood Machine introduced in the late eighteenth century, exhibits an astonishingly complex behaviour despite its simple physical description.

Its Hamiltonian formulation depends on whether or not pulleys are assumed to be massive:

- *General* Hamiltonian: defining $M_t = M + m + 2\frac{I_p}{R^2}$, $q_1 = r$, and $q_2 = \theta$:

$$\mathcal{H} = \frac{1}{2}\left(\frac{p_1^2}{M_t} + \frac{(p_2 + Rp_1)^2}{mq_1^2}\right) + gq_1\left(M - m\cos(q_2)\right) - gR\left(Mq_2 - m\sin(q_2)\right).$$

- *SAM with neglected pulleys*: assuming $m_p = I_p = R$ and $M_t = M + m$,

$$\mathcal{H}_w = \frac{1}{2}\left(\frac{p_1^2}{M_t} + \frac{p_2^2}{mq_1^2}\right) + gq_1\left(M - m\cos(q_2)\right).$$

Some background will be given during the talk on Galois theory of linear differential systems ([6]) and integrability of Hamiltonian systems ([3]). The link between these two disciplines, sometimes called *Ziglin-Morales-Ramis theory*, is the use of a family of *linear* systems $\mathrm{VE}(\Gamma) = \left\{\mathrm{LVE}_\Gamma^k : k \in \mathbb{N}\right\}$ given by the higher-order variational equations along a given particular solution Γ of a given system (whether or not Hamiltonian).

Morales' and Ramis' integrablility criterion of can be summed up, in the Hamiltonian case, in the following :

Theorem 1 (J. Morales-Ruiz & J.-P. Ramis, 2001 [4]). *Let H be an n-degree-of-freedom Hamiltonian having n meromorphic independent first integrals in pairwise involution, defined on a neighbourhood of an integral curve Γ. Then, $\mathfrak{g} := \mathrm{Lie}(\mathrm{Gal}(VE_\Gamma))$ is an abelian algebra, hence the identity component $\mathrm{Gal}(VE_\Gamma)^0$ is a* ***commutative*** *group.*

A recent extension of Theorem 1 by its authors, in an article co-written with C. Simó:

Theorem 2. *If the previous hypotheses hold, then* $\mathrm{Gal}\left(\mathrm{LVE}_\Gamma^k\right)^0$ *is commutative for all* $k \geq 1$*, and so is* $\widehat{G}^0$*, where* $\widehat{G} := \varprojlim \mathrm{Gal}\left(\mathrm{LVE}_\Gamma^k\right)$.

The intent behind this talk is to prove the non-integrability of the Hamiltonian systems $\mathcal{H}$ and $\mathcal{H}_w$ modelling SAM, using results from the incipient framework of Ziglin-Morales-Ramis theory, especially those by Boucher, Weil and Aparicio. The subsequent recollection of basics in Analytical Mechanics, Formal Calculus and Differential Algebra, as well as a number of alternative or partial proofs of the same basic result, is assembled into a comprehensive survey of algorithms (relying on symbolic rather than numerical calculations) aimed at detecting chaotic behaviour in general potential systems, especially monodromy matrices of the system's linearised higher variational equations. Hence, this is an application of Theorem 2, the recent results by Aparicio and Weil [1] and those by the three authors of the present communication [2].

References

1. Ainhoa Aparicio Monforte and Jacques-Arthur Weil. A "reduced form" for symplectic linear differential systems and its application to integrability of Hamiltonian systems. 2009.
2. Ainhoa Aparicio Monforte, Sergi Simon Estrada and Jacques-Arthur Weil, . A Prolongation Method to Compute Linearizations of First Integrals of Hamiltonian differential Systems. In *Proceedings of the MEGA (Effective methods in Algebraic Geometry)* (Barcelona, 2009).
3. Michèle Audin. *Les systèmes hamiltoniens et leur intégrabilité*, volume 8 of *Cours Spécialisés [Specialized Courses]*. Société Mathématique de France, Paris, 2001.
4. Juan J. Morales Ruiz. *Differential Galois theory and non-integrability of Hamiltonian systems*, volume 179 of *Progress in Mathematics*. Birkhäuser Verlag, Basel, 1999.
5. José-Philippe Pérez, Olivier Pujol, Jean-Pierre Ramis, Juan J. Morales-Ruiz, Carles Simó, Sergi Simon, Jacques-Arthur Weil, Swinging Atwood machine: experimental and theoretical studies. Preprint.
6. Marius van der Put and Michael F. Singer. *Galois theory of linear differential equations*, volume 328 of *Grundlehren der Mathematischen Wissenschaften [Fundamental Principles of Mathematical Sciences]*. Springer-Verlag, Berlin, 2003.